PNAS Nexus, 2024, 3, pgae390
https://doi.org/10.1093/pnasnexus/pgae390
Advance access publication 9 September 2024
Research Report

The lysogenic filamentous *Pseudomonas* bacteriophage phage Pf slows mucociliary transport

Elizabeth B. Burgener[a,b,*], Pamela C. Cai[c], Michael J. Kratochvil[d], Laura S. Rojas-Hernandez[a], Nam Soo Joo[a,e], Aditi Gupta[a], Patrick R. Secor[f], Sarah C. Heilshorn[d], Andrew J. Spakowitz[c], Jeffrey J. Wine[e], Paul L. Bollyky[g] and Carlos E. Milla[a]

[a]Department of Pediatrics, Center for Excellence in Pulmonary Biology, Stanford University, Stanford, CA 94305, USA
[b]Division of Pediatric Pulmonology and Sleep Medicine, Children's Hospital of Los Angeles, Keck School of Medicine, University of Southern California, Los Angeles, CA 90027, USA
[c]Department of Chemical Engineering, Stanford University, Stanford, CA 94305, USA
[d]Department of Materials Science and Engineering, Stanford University, Stanford, CA 94305, USA
[e]Cystic Fibrosis Research Laboratory, School of Humanities and Sciences, Stanford University, Stanford, CA 94305, USA
[f]Division of Biological Sciences, University of Montana, Missoula, MT 59812, USA
[g]Division of Infectious Diseases and Geographic Medicine, Department of Medicine, Stanford University, Stanford, CA 94305, USA
*To whom correspondence should be addressed: Email: eburgener@chla.usc.edu
Edited By Dennis Discher

Abstract

Pseudomonas aeruginosa is a major pulmonary pathogen causing chronic pulmonary infections in people with cystic fibrosis (CF). The *P. aeruginosa filamentous* and lysogenic bacteriophage, Pf phage, is abundant in the airways of many people with CF and has been associated with poor outcomes in a cross-sectional cohort study. Previous studies have identified roles for Pf phage in biofilm formation, specifically forming higher-order birefringent, liquid crystals when in contact with other biopolymers in biofilms. Liquid crystalline biofilms are more adherent and viscous than those without liquid crystals. A key feature of biofilms is to enhance bacterial adherence and resist physical clearance. The effect of Pf phage on mucociliary transport is unknown. We found that primary CF and non-CF nasal epithelial cells cultured at air–liquid interface treated with Pf phage exhibit liquid crystalline structures in the overlying mucus. On these cell cultures, Pf phage entangles cilia but does not affect ciliary beat frequency. In both these in vitro cell cultures and in an ex vivo porcine trachea model, introduction of Pf phage decreases mucociliary transport velocity. Pf phage also blocks the rescue of mucociliary transport by CF transmembrane conductance regulator modulators in CF cultures. Thus, Pf phage may contribute to the pathogenesis of *P. aeruginosa*-associated CF lung disease via induction of liquid crystalline characteristics to airway secretions, leading to impaired mucociliary transport. Targeting Pf phage may be useful in treatment CF as well as other settings of chronic *P. aeruginosa* infections.

Keywords: bacteriophage, mucociliary transport, cystic fibrosis

Significance Statement

Pf phage is a nonlytic bacteriophage of *Pseudomonas aeruginosa* found in chronic infections that creates liquid crystalline biofilms. This confers increased adhesion and viscosity to biofilms, thus making clinical infections challenging to clear. We show that Pf phage also impairs mucus transport of the airway epithelium, which is critical for defense against invading pathogens, in both a primary epithelial cell culture model and an ex vivo porcine tracheal model. Notably, Pf phage abrogates the rescue of defective mucus transport by cystic fibrosis transmembrane conductance regulator modulator drugs. This demonstrates yet another mechanism by which *P. aeruginosa* infections persist within the airway, subverting host defenses. This further highlights the potential of Pf phage as a novel therapeutic target for treating chronic *P. aeruginosa* infections.

Introduction

In cystic fibrosis (CF), defective or absent cystic fibrosis transmembrane conductance regulator (CFTR) protein results in an anion permeability defect that leads to thick and dehydrated secretions. Retained airway secretions become colonized with bacteria, establishing a cycle of inflammation and infection with progressive tissue destruction and eventual death or need for lung transplantation (1–3).

In the past decade, CF care has been transformed by highly effective CFTR modulator therapies, drugs that target defective CFTR protein and restore its function (4). These medications significantly improve mucociliary transport (5) and induce dramatic

Competing Interest: The authors declare no competing interests.
Received: May 13, 2024. **Accepted:** August 20, 2024

improvements in lung function and quality of life (6). However, even with these groundbreaking therapies, airway inflammation and infection persist, notably infection with *Pseudomonas aeruginosa* (*P. aeruginosa*) (7–10).

P. aeruginosa is a common pathogen infecting the airways of people with CF and is associated with accelerated decline in lung function and mortality (11–14). A significant effort is placed in preventing acquisition of *P. aeruginosa* and attempting eradication after initial detection (15–17). However, *P. aeruginosa* forms biofilms that facilitate persistence of the bacteria in the airway (18–20). Consequently, a significant proportion of people with CF are chronically infected by the time they reach adulthood (21).

The lysogenic filamentous bacteriophage, Pf phage, infects *P. aeruginosa* and incorporates into the bacterial chromosome as a prophage. Pf phage expression and production are significantly increased in the biofilm growth state (22–24). Unlike lytic bacteriophage, Pf phage does not lyse *P. aeruginosa* upon replication; instead, long filamentous virions are extruded from the bacteria without killing it (25). Pf phage can be highly abundant in CF sputum, at concentrations up to 10^{10} virions/mL (26, 27). We have previously shown that the presence of Pf phage in the sputum is associated with poor outcomes in a cross-sectional study of people with CF (27).

In vitro Pf phage contributes to *P. aeruginosa* biofilm formation by assembling biofilms and polymers commonly present in the CF airway (DNA, mucins, actin, and alginate produced by mucoid *P. aeruginosa*) into a liquid crystalline structure (26). This higher-order structure is spontaneously created by crowding (depletion) forces between Pf phage virions and polymers, providing additional adhesion and viscosity to *P. aeruginosa* biofilms (28). The impact of Pf phage-induced liquid crystals on mucociliary clearance is unknown.

We hypothesized that Pf phage carriage would provide a selective advantage to *P. aeruginosa* by disrupting clearance from the airway by impairing mucociliary transport. First, we demonstrate liquid crystalline structures in epithelial cell culture mucus treated with Pf phage. Then, we demonstrate both in vitro and in an ex vivo model that Pf phage slows mucociliary transport. Our data provide support for a role of Pf phage in the pathogenicity of *P. aeruginosa* and as a novel therapeutic target for chronic *P. aeruginosa* airway infection.

Results

Pf phage organizes mucus in ways that entangle cilia in an in vitro culture system

Direct visualization of the apical surface of primary CF nasal epithelial cell cultures at air–liquid interface (ALI) treated with Pf phage by polarized light microscopy demonstrated areas of birefringent liquid crystal along the ciliated surface (Fig. S1A), while no birefringence was seen in the negative, wild-type (WT) cultures (Fig. S1B). Additionally, mucus collected from the apical surface of the Pf phage-treated culture also revealed crystalline structures (Fig. S1C), which demonstrate areas of birefringence (Fig. S1D). These findings are consistent with Pf phage organizing the apical mucus into high-order birefringent, liquid crystalline structures (28).

We obtained additional details by scanning electron microscopy (SEM) imaging in both WT (Fig. 1A and B) and CF (Fig. 1C and D) cultures. Matting and clumping of cilia with visible net-like structures were observed in both WT and CF cultures exposed to Pf phage (Fig. 1B and D). Together, these data suggest that Pf phage interacts with the mucin polymers and induces the formation of structures that in contact with the cilia produce an entangling effect. This observed adherence of Pf phage to the cilia is consistent with the biophysical properties we have described previously in Pf phage liquid crystals (26, 28).

Pf phage slows mucociliary transport and blocks rescue by CFTR modulators

To determine the effects of the Pf phage-induced entanglement of the ciliated surface on mucociliary function, we applied Pf phage to the apical surface of the nasal epithelial cell cultures at ALI. While ciliary beat frequency is significantly slower in CF vs. WT cultures, we found that ciliary beat frequency is not affected in a consistent manner by Pf phage in WT and CF cells (Fig. 2A), including those that were treated with the combination of CFTR modulators: elexacaftor, tezacaftor, and ivacaftor (ETI), to rescue CFTR function (Fig. 2B). There was no difference in active area of ciliary beating between all conditions (Fig. 2C).

However, when we measured mucus transport at the apical surface, we found a significant impairment of transport in the presence of Pf phage. The mucociliary transport was dramatically decreased in the presence of Pf phage in WT cell cultures (Figs. 3A and S2–S3). There was no significant decrease in the CF cell cultures as the control CF cultures started with very low mucociliary transport velocities. However, the lower velocity seen in CF cells was rescued by ETI treatment, but this effect was abrogated by the presence of Pf phage (Fig. 3B).

We conducted additional experiments to evaluate other phage including the *Escherichia coli* filamentous phage, Fd, which is very similar in structure to Pf phage, and a lytic *P. aeruginosa* phage, DMS3vir, and found that they also decreased mucociliary transport but less dramatically than Pf phage (Fig. 3C).

Further, by multiple particle tracking analysis of both WT cultures, both effective diffusivity (Fig. 3D) and mean squared distance (Fig. 3E) of particle transport were significantly decreased by the presence of Pf phage.

These data demonstrate that the effect of Pf phage on mucociliary transport is not due to slowing of ciliary beat frequency, but rather to an impediment to the mobilization of the mucus on the epithelial surface.

Pf phage impacts mucociliary transport in ex vivo newborn piglet trachea treated with Pf phage

To translate our findings, we sought to test the effects of Pf phage on a validated ex vivo system for assessing mucociliary transport. To this end, we made use of our previously reported method to measure mucociliary transport velocity (MCV) in explanted newborn piglet tracheas (29) (Fig. 4A).

Monitoring the cephalad particle movement recorded over 30 minutes, we observed that MCV in Pf phage-treated tracheas was significantly lower ($P = 0.03$) than control conditions ($n = 4$ piglet tracheas per condition) (Figs. 4B, C and S4A, B). These data establish that Pf phage impairs mucociliary transport when present in the mucosal surface of an intact airway.

Discussion

We have identified impacts of Pf phage on mucociliary transport. We previously reported that Pf phage promotes higher-order crystalline structures in mixtures of biologically relevant polymers (26, 28, 30). We now report that Pf phage-induced crystalline structures directly entangle respiratory cilia and impair mucociliary transport in primary epithelial cell culture as well as an ex vivo

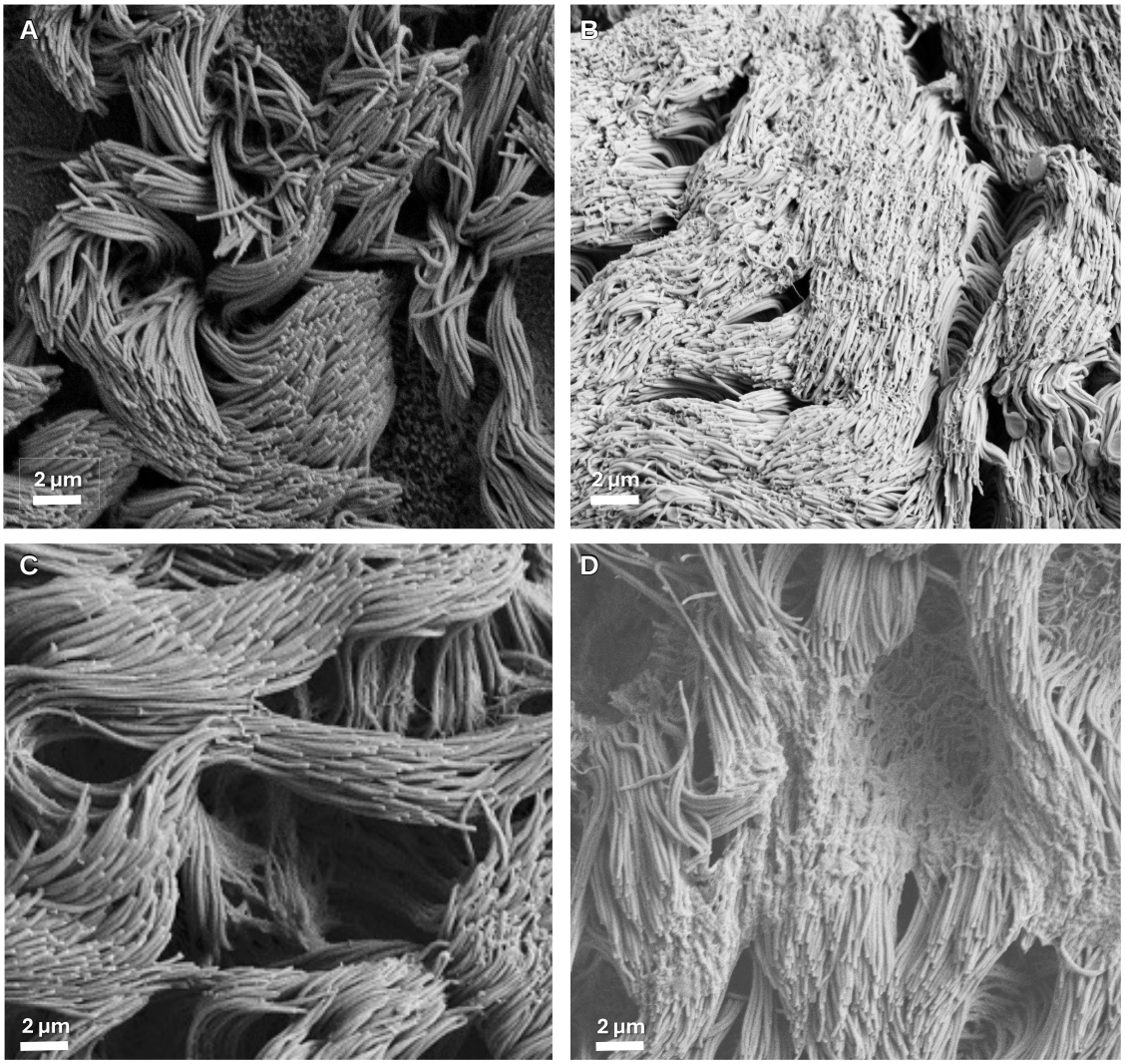

Fig. 1. Pf forms aggregates that entangle the cilia. SEM imaging (12,000×) of WT human nasal epithelial culture (HNEC) at ALI treated with apical PBS (A) or Pf (B) and of CF HNEC at ALI similarly treated with apical PBS (C) or Pf (D).

porcine trachea model. These findings provide additional mechanistic insight into how Pf phage may impact lung disease in CF and potentially in other clinical settings.

The effects of Pf phage on mucociliary transport are consistent with our previous work of demonstrating Pf phage-induced liquid crystals (26, 28, 30). Here, we demonstrate Pf phage is capable of forming liquid crystalline structures within mucus that adheres to the cell culture surface and the SEM images reveal Pf phage entangling ciliary axonemes (Fig. 1B and D). Interestingly, in the epithelial cell cultures we find ciliary beat frequency is not affected by Pf phage (Fig. 2). This suggests that the liquid crystal may increase mucus viscosity and adhesiveness and thus effectively become anchored on the mucosal surface rendering the ciliary beat ineffective at mobilizing the mucus. This is supported by the negative effects found on MCV by adding Pf phage in both our in vitro and ex vivo systems (Figs. 3 and 4).

There is precedent for interactions of bacteriophage with polymers on mucosal surfaces from prior work identifying attachment of bacteriophage capsids to mucus (31). This is postulated to be a mechanism evolved by bacteriophage as a predator to take advantage of the mucosal surface to gain increased exposure to potential bacterial prey and may explain the similar yet less dramatic effect noted with DMS3vir, a tailed lytic *P. aeruginosa* bacteriophage (Fig. 3C). The highly polymeric nature of CF airway secretions likely allows Pf phage to form liquid crystalline structures that are highly adherent within the airway (26). This we postulate serves as an additional mechanism that *P. aeruginosa* utilizes to persist as a well-established biofilm within the CF airway.

Perhaps of greatest interest for clinicians treating individuals with CF, the presence of Pf phage abrogates the normalization of mucociliary transport in the CF cultures treated with the highly effective CFTR modulator, ETI (Fig. 3B). Whether the effects observed in the CF condition can be reverted simply by exchanging for WT-like mucus (i.e. similar solids concentrations) is answered by our experiment with ETI-treated cells. ETI has been shown in similar in vitro cultures to have a significant effect on mucus properties (32). We then find that under this WT-like mucus conditions, Pf still has a negative effect on mucociliary transport and negates the positive effects of ETI, with the mucociliary transport velocities similar to that of CF cultures without ETI treatment. This suggests that for individuals with chronic *P. aeruginosa* infection being treated with ETI, the presence of Pf phage may affect their ability to clear *P. aeruginosa* from their airways. Given recent data demonstrating persistence of *P. aeruginosa* among a

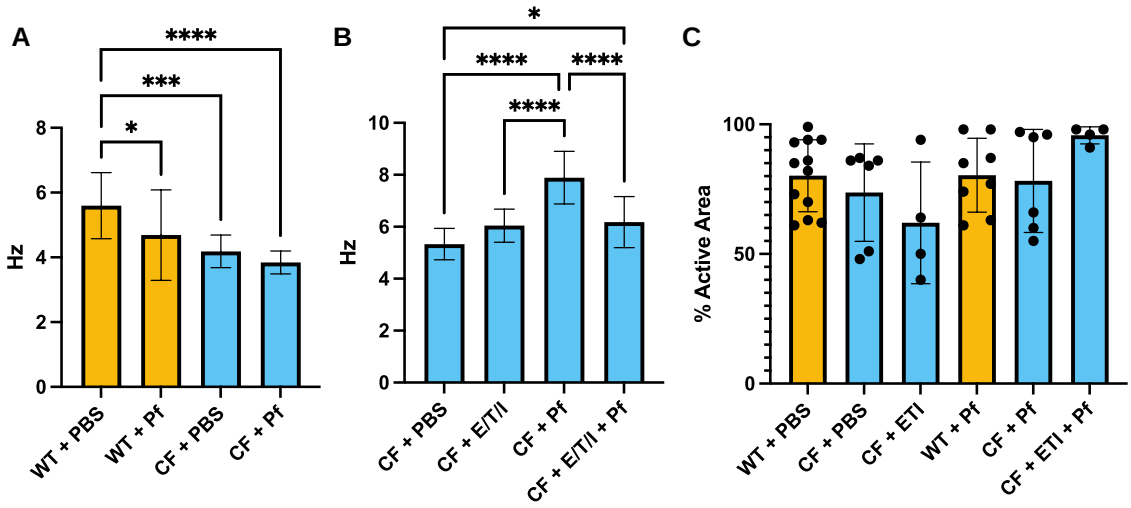

Fig. 2. Ciliary beat frequency of human nasal epithelial cell cultures at ALI in the presence of pf phage. Ciliary beat frequency measured by video microscopy on A) WT and CF primary cells treated with either Pf phage or of control of PBS, and B) F508del homozygous donor cells were pretreated with ETI or PBS daily for 48 hours and then treated with Pf phage or PBS. C) Percent active area per imaged field of ALI culture insert for each condition. Analysis by one-way ANOVA with Tukey's multiple comparison (A to C). Unmarked comparisons are not significant. *P*-value = * < 0.05; ** < 0.01; *** < 0.001; **** < 0.0001. E/T/I, elexacaftor/tezacaftor/ivacaftor; WT, wild type.

proportion of individuals with CF treated with ETI (9, 10), it will be important to further investigate the implications of Pf phage in the CF airway in future studies.

There are limitations to this study. First, our in vitro systems do not permit full exploration of the effects of Pf phage in the presence of *P. aeruginosa* and biofilms or in the presence of immune cells. While the CF airway environment is quite complex and heterogeneous, here we aimed to interrogate primarily the effect of Pf phage in its interaction with the mucociliary system. Thus, our experimental procedures as described allowed us to isolate the effects of Pf phage more clearly. Second, our ex vivo model does not include all the components of an intact organ, but for all practical purposes has demonstrated to be of great value to identify important changes in mucociliary transport. Whether these effects translate directly to the CF airway will require further studies in intact animal models of chronic airway infection. These aspects are the focus of current efforts.

In summary, we find that the *P. aeruginosa* bacteriophage, Pf phage, forms liquid crystals in the mucus on airway cultures and slows mucociliary transport in two airway models. Together with work published by our group and others, demonstrating effects of Pf phage also on bacterial fitness (22, 33–36), antibiotic tolerance (26, 27, 30, 37, 38), and host immunity (30, 39), these data suggest that Pf phage promotes chronic infection in multiple ways. Here, we identify an additional mechanism that *P. aeruginosa* may utilize to persist in the CF airway, as well as identifying Pf phage as a potential therapeutic target to control chronic *P. aeruginosa* infections. These results may be relevant to diseases outside of CF where *P. aeruginosa* infections are problematic, such as ventilator-associated pneumonia, tracheostomy-associated airway infection, bronchiectasis, and primary ciliary dyskinesia, among others.

Materials and methods

Human nasal epithelial cells

Nasal epithelial cells were obtained from pwCF and WT, healthy controls by brushing both inferior turbinates and following an established standard operating procedure. The CF cells were obtained from a 14-year-old male patient with 3876delA (p.Lys1250ArgfsX9 or c.3744delA)/3876delA (p.Lys1250ArgfsX9 or c.3744delA) mutations for the experiments in Figs. 2A and 3A and C. Additional cells were obtained from an 18-year-old female with F508del (p.Phe508del or c.1521_1523del)/F508del (p.Phe508 del or c.1521_1523del) mutations for the experiments in Figs. 2A and 3B as they would be responsive to ETI. The WT cells were obtained from a 60-year-old healthy male volunteer with known WT CFTR. This project was approved by the Stanford University IRB protocol (protocol #37232). Informed consent was obtained from all subjects.

Human nasal epithelial cell cultures at ALI

Human nasal epithelial cells were cultured at ALI as per previously published protocol (40, 41). Briefly, the cells from the nasal sample were dissociated, seeded onto collagen-coated, 0.4-μm pore polyester membrane inserts (Corning Inc.), and expanded with PneumaCult Ex-Plus media (StemCell Technologies) added to both the basal and apical chambers (42). Once cells reached confluence, an ALI was generated by removing the apical medium and replacing the basal medium with PneumaCult ALI media (StemCell Technologies). Once cultures were fully ciliated and active mucociliary activity was visualized, typically after 3 weeks, we proceeded to experimental measurements. For the CF cultures with ETI-responsive mutations, rescue CFTR function was introduced by treatment with a combination of elexacaftor 3 μM and tezacaftor 3 μM for 48 hours prior to and supplemented by the addition of ivacaftor 10μM at time of measurements. All inserts were washed with warm phosphate-buffered saline (PBS) to the apical surface to remove mucus and debris 48 hours prior to experimental manipulations as we have described before (43). Pf phage or vehicle control was then applied to the apical surface at a final concentration of 10^9 virions/mL and incubated at 37 °C for 24 hours prior to imaging. Once in vitro experiments were completed, filter inserts were either imaged with polarized light microscopy to evaluate for birefringence or fixed in 4% glutaraldehyde in cacodylate buffer for SEM.

Scanning electron microscopy

For imaging of ALI culture inserts by SEM, we followed our published methods (40). In brief, Transwell filters were fixed by

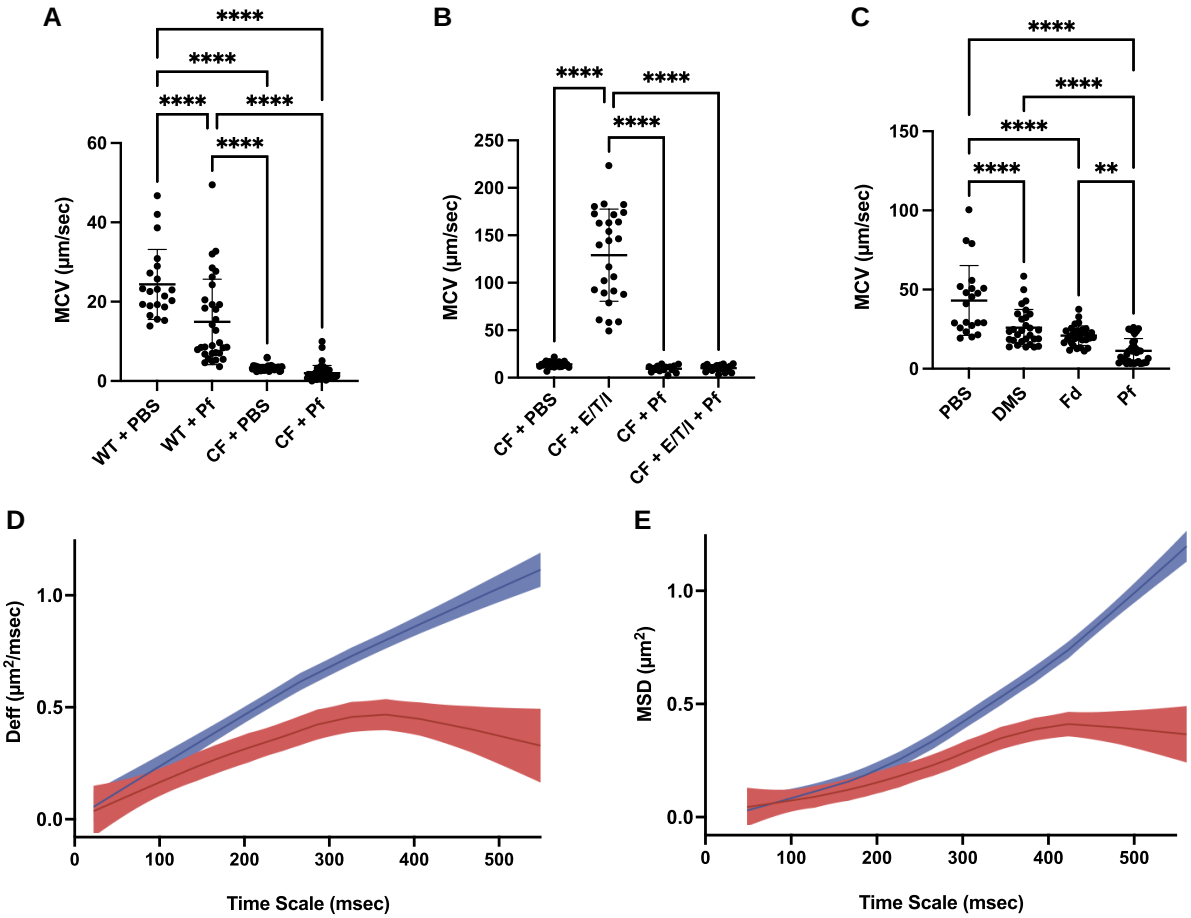

Fig. 3. Mucus transport velocity of human nasal epithelial cell cultures at ALI in the presence of pf phage. MCV was measured by video monitoring of beads placed on top of epithelial cells at ALI culture. A) CF and WT nasal epithelial cells grown at ALI were treated with Pf phage or PBS depicted as mean bead velocity as a measure of MCV. B) CF cells with PBS, Pf phage, and/or E/T/I (given as pretreatment 48 hours prior to phage treatment). C) WT cells treated with PBS, Pf phage, control phage Fd, or control phage DMSvir3. Analysis by Kruskal–Wallis with Dunn's multiple comparison tests for individual comparisons (A and B) and one-way ANOVA with Tukey's multiple comparison (A to C). *P*-value * < 0.05; ** < 0.01; *** < 0.001; **** < 0.0001. Multiple particle tracking performed on WT cultures represented by D) ensemble effective diffusivity and E) ensemble mean square distance, over a range of time scales from 10 to 500 ms demonstrate a substantial decrease in the active transport of beads across the epithelial surface reflecting an impairment of the mucociliary active transport mechanism. The shaded area represents 95% CIs. Blue = PBS treated and red = Pf phage treated. Videos of particle tracking are included in Figs. S2 and S3. Deff, ensemble effective diffusivity; DMS, DMS3vir phage; E/T/I, elexacaftor/tezacaftor/ivacaftor; Fd, Fd phage; MSD, ensemble mean squared distance; PBS, phosphate-buffered saline; WT, wild type.

submersion in a fixative mix of 2% glutaraldehyde, 4% paraformaldehyde in 0.1 M Na-cacodylate buffer titrated to pH 7.4, and kept at 4 °C overnight. The samples were osmicated, dehydrated, and then dried with a Tousimis AutoSamdri-815 critical point dryer. The samples were mounted luminal side up and sputter-coated with 100Å layer of Au/Pd. Images were acquired with a Hitachi S-3400N VP-SEM microscope operated at 10–15 kV, with a working distance of 7–10 mm and using secondary electron detection.

In vitro ciliary beat frequency and MCV of human nasal epithelial cell cultures at ALI

Once the ALI cultures had reached full maturity as evidenced by the presence of active ciliary beat, inserts were washed as noted above and then imaged at 500× on an inverted microscope with a heated stage with controlled environmental conditions at 37 °C and at a frame rate of 120 fps (Basler Ace, Basler AG, Germany). The images were acquired and analyzed with the SAVA system (Ammons Engineering, Clio, MI, USA) to determine ciliary beat frequency. Five regions were evaluated per filter insert and ciliary beat frequency averaged. Next, the inserts were cut from their support, placed on a concave well slide filled with media so that only the basal side was exposed to media, and 20 µL of a 0.1% suspension of 2-µm fluorescent polystyrene beads (Thermo Scientific R0200) was added to the apical surface. The slide was then placed on a custom-built system that includes a heated stage at 37 °C and imaged from above with a digital microscope fitted with a high-speed camera (Keyence Inc., Elmwood Park, NJ, USA). The images were acquired on three regions per filter and with tracking of 10–20 beads per region at a frame rate of 1,000 fps. Image files were exported to ImageJ to analyze particle movement with the MTrackJ plug-in (v. 1.5.1) (44). The extracted frame-by-frame coordinates were then used to estimate individual particle distance traveled and MCV. In addition, the coordinates and time lag between frames were used to define time scales (τ) following multiple particle transport methodology (45) and then determine the mean squared displacement of the particle for all possible time durations. The effective diffusivity (Deff) was then calculated from the mean squared displacement and time scales extracted (45). The mean squared displacement and effective diffusivity data generated for all particles tracked

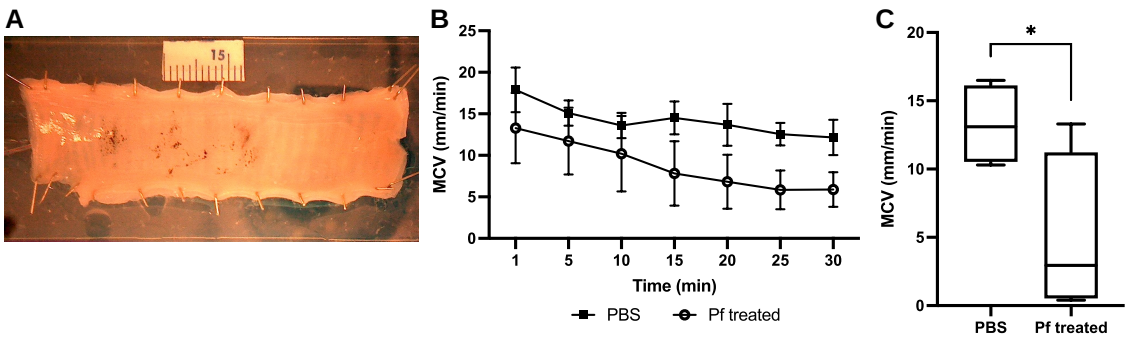

Fig. 4. MCV in ex vivo newborn piglet trachea treated with Pf phage. MCV measurement performed by tracking of ink toner particles and sequential imaging over 30 minutes. The setup of the ex vivo trachea is depicted in (A). Pf phage added at A concentration of 10^{10}/mL. Control treated with comparable volume of PBS. Both conditions treated with 0.3 μM carbachol and 10 μM formoterol for maximal mucociliary transport.(39) Tracking was initiated 30 minutes after treatments applied, and images were automatically captured every 5 minutes (four images/20 s intervals) using a digital camera. B) Time course of first 30 minutes of recorded MCV in pig tracheas ($n = 4$ per condition). Control in open circles and Pf phage-treated in solid squares ($P = 0.04$ for difference between treatments). C) Boxplots with the average MCV over 30 minutes, mean (*) $T_{10–90}$ MCV (in millimeter per minute): control 13.2 ± 0.2; Pf 8.2 ± 0.5 ($P = 0.0462$). Statistical comparison by *t* test. *P*-value * < 0.05. MCV, mucociliary transport velocity; PBS, phosphate-buffered saline; Pf, Pf phage.

under Pf + and Pf− conditions were analyzed by Loess-smoothed regression to generate ensemble plots of mean squared displacement and effective diffusivity vs. time scales with 95% CIs to allow for comparisons between Pf+ and Pf− conditions.

MCV measurement in ex vivo piglet trachea

Tracheas from WT, Yorkshire, newborn piglets (2–5 days old) were freshly obtained from the swine facility at UC Davis. All methods using animal tracheae were carried out in accordance with relevant guidelines and regulations of Stanford University, and animal protocols received institutional approval (Stanford IACUC protocol # 10048). Piglet tracheas were transported in cold PhysioSol (Hospira Inc, IL, USA) and then transferred to ice-cold Krebs-Ringer bicarbonate (KRB) buffer gassed with 95% O_2 and 5% CO_2 and kept at 4 °C until use. The KRB buffer contained (in mM) 115 NaCl, 25 $NaHCO_3$, 2.4 K_2HPO_4, 0.4 KH_2PO_4, 1.2 $MgCl_2$, 1.2 $CaCl_2$, 10 glucose, and 1.0 μM indomethacin, adjusted to pH 7.2 and ~290 mOsm at room temperature. Indomethacin was added to reduce tissue exposure to endogenously released prostaglandins.

Measurement of MCV was taken as we have previously reported (46–48). Briefly, each whole-length piglet trachea was cut open along the mid-dorsal line and mounted mucosal side up onto a Sylgard elastomer platform. The prepared trachea was placed into a sealed, humidified chamber bubbled continuously with gas (95% O_2/5% CO_2) with the serosal surface bathed with KRB buffer. For the initial 30-minute stabilization period, the tissue was submerged in the bath as the temperature was gradually increased to 37 °C. Then. excess apical and bath solution was drained. The tissue was then stimulated for 30 minutes with the combined application of cholinergic (0.3 μM carbachol) and β-adrenergic (10 μM formoterol) applied to the serosal bath to initiate mucus secretion from submucosal glands and surface epithelia (46) in the presence of apical Pf phage (~1 mL of 10^{10} Pf phage virions/mL in PBS or PBS as a control) designed to maximize contact between secreted mucus and apically added Pf phage. After 30-minute mucosal incubation, the excessive mucosal Pf phage was drained, and bath was refreshed with the combined agonists. After additional 10-minute stabilization period, MCV measurements using time-lapse imaging began by placing dry Xerox ink particles (~10 μm) apically on the caudal end. The images of cephalad particle movements were automatically captured (four images at 20-second intervals every 5 min) by an Aven time-lapse digital camera and associated software (Ann Arbor, MI, USA). MCV (in millimeter per minute) was determined by measuring the fastest moving group of particles using NIH ImageJ software (46).

Phage purification and quantification

Pf4 phage was isolated and purified from PA01, DMS3vir from PA14 and Fd phage from *E. coli*. Phage purification was performed as previously described (30). Briefly, bacteria at mid-log phase growth were infected with stocks of phage and cultured in LB broth for 48 hours at 37 °C in a shaking incubator. Centrifugation at 6,000×*g* for 5 minutes was performed to remove bacteria. The supernatant was treated with 1 μg/mL DNase (Roche, catalog # 4716728001) for 2 hours at 37 °C, followed by treatment with 250 μg/mL of RNAse A (Thermo Fisher Scientific, catalog # EN0531) for 4 hours at 37 °C. Vacuum filtration through a 0.22-μM filter was performed to sterilize supernatant. Pf4 phage was precipitated from the supernatant by adding 0.3 M NaCl and 4% polyethylene glycol (PEG) 8000 (Millipore Sigma, catalog # P2139). Phage solutions were incubated overnight at 4 °C. Phage was then pelleted by centrifugation at 10,000×*g* for 20 minutes. The supernatant was subjected to a second round of PEG precipitation as above. The purified phage pellets were suspended in sterile PBS and dialyzed in 10-kDa molecular weight cut off tubing (Fisher Scientific, catalog # 88243) against PBS and quantified by plaque assay, and Pf phage preparation titers were confirmed by qPCR using our previously described methods (26, 30, 49).

Statistical analyses

Graphing and statistical analyses were performed using GraphPad Prism 6 (GraphPad Software), R (R Computing), and SAS (v.9.4, SAS Institute Cary, NC, USA). Comparisons of ciliary beat frequency and MCV by particle tracking were made by one-way ANOVA with Tukey's adjustment of multiple comparisons for individual comparisons. Comparison of average MCV in porcine model was based on simple two-sample *t* test.

Supplementary Material

Supplementary material is available at *PNAS Nexus* online.

Funding

E.B.B. was supported by the National Heart, Lung, and Blood Institute of the National Institue of Health (T32HL129970, 1K23HL 169902-01), the Francis Family Foundation (Parker B Franis Fellowship), and the Cystic Fibrosis Foundation (BURGEN20Q0, BURGEN21A0-KU). P.C.C. was funded by a National Science Foundation (Graduate Research Fellowship). A.J.S. was supported by the National Science Foundation (Physics of Living Systems Program) (PHY-2102726). N.S.J. was funded by the Cystic Fibrossis Foundation (JOO19G0). P.L.B. was supported by National Institutes of Health (R01AI138981, K24AI166718-01A1, and R21GM147838) and a grant from the Emerson Collective. P.R.S. was supported by National Institutes of Health (R01AI138981). C.E.M. was supported by grants from the Cystic Fibrosis Foundation (MILLA22Y0, MILLA23P0), the National Heart, Lung, and Blood Institute (1R01HL148184), and the Ross Mosier Laboratories Gift Fund.

Author Contributions

Conceptualization of study and individual experiments by E.B.B., P.C.C., M.J.K., P.R.S., S.C.H., A.J.S., P.L.B., and C.E.M. Collection of data and performance of experiments by E.B.B., N.S.J., L.S.R.-H., A.G., and C.E.M. Analysis of data E.B.B., N.S.J., P.C.C., M.J.K., J.J.W., P.L.B., and C.E.M. Editing of manuscript E.B.B., L.S.R.-H., N.S.J., P.C.C., M.J.K., A.G., P.R.S., S.C.H., A.J.S., J.J.W., P.L.B., and C.E.M.

Data Availability

All data are included in Tables S1 and S2.

References

1 Stoltz DA, Meyerholz DK, Welsh MJ. 2015. Origins of cystic fibrosis lung disease. *N Engl J Med*. 372(4):351–362.
2 Khan T, *et al.* 1995. Early pulmonary inflammation in infants with cystic-fibrosis. *Am J Respir Crit Care Med*. 151(4):1075–1082.
3 Hoegger MJ, *et al.* 2014. Impaired mucus detachment disrupts mucociliary transport in a piglet model of cystic fibrosis. *Science*. 345(6198):818–822.
4 Van Goor F, *et al.* 2006. Rescue of ΔF508-CFTR trafficking and gating in human cystic fibrosis airway primary cultures by small molecules. *Am J Physiol Lung Cell Mol Physiol*. 290(6):L1117–L1130.
5 Donaldson SH, *et al.* 2023. Effect of elexacaftor/tezacaftor/ivacaftor on mucus and mucociliary clearance in cystic fibrosis. *J Cyst Fibros*. 23(1):155–1601.
6 Ong T, Ramsey BW. 2023. Cystic fibrosis: a review. *JAMA*. 329(21): 1859–1871.
7 Hisert KB, *et al.* 2017. Restoring cystic fibrosis transmembrane conductance regulator function reduces airway bacteria and inflammation in people with cystic fibrosis and chronic lung infections. *Am J Respir Crit Care Med*. 195(12):1617–1628.
8 Heltshe SL, Rowe SM, Skalland M, Baines A, Jain M. 2017. GOAL investigators of the cystic fibrosis foundation therapeutics development network. Ivacaftor-treated CF patients derive long-term benefit despite no short-term clinical improvement. *Am J Respir Crit Care Med.*, 197(11):1483–1486.
9 Nichols DP, *et al.* 2023. Pharmacologic improvement of CFTR function rapidly decreases sputum pathogen density but lung infections generally persist. *J Clin Invest*. 133(10):e167957.
10 Armbruster CR, *et al.* 2024. Persistence and evolution of *Pseudomonas aeruginosa* following initiation of highly effective modulator therapy in cystic fibrosis. *mBio*. 15(5):e00519–e00524.
11 Emerson J, Rosenfeld M, McNamara S, Ramsey B, Gibson RL. 2002. *Pseudomonas aeruginosa* and other predictors of mortality and morbidity in young children with cystic fibrosis. *Pediatr Pulmonol*. 34(2):91–100.
12 Konstan MW, *et al.* 2007. Risk factors for rate of decline in forced expiratory volume in one second in children and adolescents with cystic fibrosis. *J Pediatr*. 151(2):134–139.e1.
13 Nixon GM, *et al.* 2001. Clinical outcome after early *Pseudomonas aeruginosa* infection in cystic fibrosis. *J Pediatr*. 138(5):699–704.
14 Rosenfeld M, *et al.* 2001. Early pulmonary infection, inflammation, and clinical outcomes in infants with cystic fibrosis*. *Pediatr Pulmonol*. 32(5):356–366.
15 Döring G, Flume P, Heijerman H, Elborn JS. 2012. Treatment of lung infection in patients with cystic fibrosis: current and future strategies. *J Cyst Fibros*. 11(6):461–479.
16 Mogayzel PJ, *et al.* 2014. Cystic fibrosis foundation pulmonary guideline. Pharmacologic approaches to prevention and eradication of initial *Pseudomonas aeruginosa* infection. *Ann Am Thorac Soc*. 11(10):1640–1650.
17 Vidya P, *et al.* 2016. Chronic infection phenotypes of *Pseudomonas aeruginosa* are associated with failure of eradication in children with cystic fibrosis. *Eur J Clin Microbiol Infect Dis*. 35(1):67–74.
18 FitzSimmons SC. 1993. The changing epidemiology of cystic fibrosis. *J Pediatr*. 122(1):1–9.
19 Costerton JW, Stewart PS, Greenberg EP. 1999. Bacterial biofilms: a common cause of persistent infections. *Science*. 284(5418): 1318–1322.
20 Parsek MR, Singh PK. 2003. Bacterial biofilms: an emerging link to disease pathogenesis. *Annu Rev Microbiol*. 57(1):677–701.
21 2020 Patient Registry Annual Data Report | Cystic Fibrosis Foundation. [accessed 2022 May 2]. https://www.cff.org/sites/default/files/2021-10/2019-Patient-Registry-Annual-Data-Report.pdf.
22 Rice SA, *et al.* 2009. The biofilm life cycle and virulence of *Pseudomonas aeruginosa* are dependent on a filamentous prophage. *ISME J*. 3(3):271–282.
23 Whiteley M, *et al.* 2001. Gene expression in *Pseudomonas aeruginosa* biofilms. *Nature*. 413(6858):860–864.
24 Knezevic P, Voet M, Lavigne R. 2015. Prevalence of Pf1-like (pro) phage genetic elements among *Pseudomonas aeruginosa* isolates. *Virology*. 483:64–71.
25 Secor PR, *et al.* 2020. Pf bacteriophage and their impact on *Pseudomonas virulence*, mammalian immunity, and chronic infections. *Front Immunol*. 11:244.
26 Secor PR, *et al.* 2015. Filamentous bacteriophage promote biofilm assembly and function. *Cell Host Microbe*. 18(5):549–559.
27 Burgener E, *et al.* 2019. Filamentous bacteriophages are associated with chronic *Pseudomonas* lung infections and antibiotic resistance in cystic fibrosis. *Sci Transl Med*. 11(488). https://doi.org/10.1126/scitranslmed.aau9748.
28 Secor PR, *et al.* 2015. Biofilm assembly becomes crystal clear—filamentous bacteriophage organize the *Pseudomonas aeruginosa* biofilm matrix into a liquid crystal. *Microbial cell (Graz, Austria)*. 3(1):49–52.
29 Wine JJ. 2010. The development of lung disease in cystic fibrosis pigs. *Sci Transl Med*. 2(29):29ps20-29ps20.
30 Sweere JM, *et al.* 2019. Bacteriophage trigger antiviral immunity and prevent clearance of bacterial infection. *Science*. 363(6434): eaat9691.

31 Barr JJ, *et al.* 2013. Bacteriophage adhering to mucus provide a non–host-derived immunity. *Proc Natl Acad Sci U S A.* 110(26): 10771–10776.

32 Morrison CB, *et al.* 2022. Treatment of cystic fibrosis airway cells with CFTR modulators reverses aberrant mucus properties via hydration. *Eur Respir J.* 59(2):2100185.

33 Penner JC, *et al.* 2016. Pf4 bacteriophage produced by *Pseudomonas aeruginosa* inhibits *Aspergillus fumigatus* metabolism via iron sequestration. *Microbiology (Reading, England).* 162(9):1583–1594.

34 Webb JS, Lau M, Kjelleberg S. 2004. Bacteriophage and phenotypic variation in *Pseudomonas aeruginosa* biofilm development. *J Bacteriol.* 186(23):8066–8073.

35 Schmidt AK, *et al.* 2024. Targeted deletion of Pf prophages from diverse Pseudomonas aeruginosa isolates has differential impacts on quorum sensing and virulence traits. *J Bacteriol.* 206(5): e0040223.

36 Schmidt AK, *et al.* 2022. A filamentous bacteriophage protein inhibits type IV pili to prevent superinfection of *Pseudomonas aeruginosa*. *mBio.* 13(1):e02441-21.

37 Tarafder AK, *et al.* 2020. Phage liquid crystalline droplets form occlusive sheaths that encapsulate and protect infectious rod-shaped bacteria. *Proc Natl Acad Sci U S A.* 117(9):4724–4731.

38 Böhning J, *et al.* 2023. Biophysical basis of filamentous phage tactoid-mediated antibiotic tolerance in *P. aeruginosa*. *Nat Commun.* 14(1):8429.

39 Popescu MC, *et al.* 2024. The Inovirus Pf4 triggers antiviral responses and disrupts the proliferation of airway basal epithelial cells. *Viruses.* 16(1):165.

40 Vladar EK, Nayak JV, Milla CE, Axelrod JD. 2016. Airway epithelial homeostasis and planar cell polarity signaling depend on multiciliated cell differentiation. *JCI insight.* 1(13):e88027.

41 Vaidyanathan S, *et al.* 2020. High-Efficiency, selection-free gene repair in airway stem cells from cystic fibrosis patients rescues CFTR function in differentiated epithelia. *Cell Stem Cell.* 26(2): 161–171.e4.

42 Vladar EK, Brody SL. 2013. Chapter fourteen—analysis of ciliogenesis in primary culture mouse tracheal epithelial cells. In: Marshall WF, editors. *Methods in enzymology*. Vol. 525. Academic Press. p. 285–309. (Cilia, Part B). https://www.sciencedirect.com/science/article/pii/B9780123979445000146.

43 Vladar EK, *et al.* 2023. Notch signaling inactivation by small molecule γ-secretase inhibitors restores the multiciliated cell population in the airway epithelium. *Am J Physiol Lung Cell Mol Physiol.* 324(6):L771–L782.

44 Meijering E, Dzyubachyk O, Smal I. 2012. Methods for cell and particle tracking. *Methods Enzymol.* 504:183–200.

45 Valentine MT, *et al.* 2001. Investigating the microenvironments of inhomogeneous soft materials with multiple particle tracking. *Phys Rev E.* 64(6):061506.

46 Joo NS, *et al.* 2021. Combined agonists act synergistically to increase mucociliary clearance in a cystic fibrosis airway model. *Sci Rep.* 11(1):18828.

47 Joo NS, Jeong JH, Cho H-J, Wine JJ. 2016. Marked increases in mucociliary clearance produced by synergistic secretory agonists or inhibition of the epithelial sodium channel. *Sci Rep.* 6(1):36806.

48 Jeong JH, Joo NS, Hwang PH, Wine JJ. 2014. Mucociliary clearance and submucosal gland secretion in the ex vivo ferret trachea. *Am J Physiol Lung Cell Mol Physiol.* 307(1):L83–L93.

49 Burgener EB, *et al.* 2020. Methods for extraction and detection of pf bacteriophage DNA from the sputum of patients with cystic fibrosis. *PHAGE.* 1(2):100–108.